Bull. Chem. Soc. Ethiop. **2024**, 38(5), 1311-1327.
DOI: https://dx.doi.org/10.4314/bcse.v38i5.10

ISSN 1011-3924
Printed in Ethiopia
Online ISSN 1726-801X

SPECTROPHOTOMETRIC, QUANTUM CHEMICAL AND MOLECULAR DOCKING INVESTIGATIONS OF 4*H*-1-BENZOPYRAN-DERIVED Pd(II) COMPLEXES

Tanu Arora[1], Km Garima[2], Vikas Kumar[3], Saleem Javed[4], Mohammad Azam[5], Saud I. Al-Resayes[5] and Nivedita Agnihotri[1*]

[1]Department of Chemistry, Maharishi Markandeshwar (Deemed to be University), Mullana, Ambala-133207, India
[2]Department of Chemistry, CMP College, University of Allahabad, Prayagraj-211002, India
[3]Department of Microbiology, International Medical School, University of International Business, Almaty, Kazakhstan
[4]Department of Chemistry, Jamia Millia Islamia, New Delhi, India
[5]Department of Chemistry, College of Sciences, King Saud University, P.O. Box: 2455, Riyadh 11451, Saudi Arabia

(Received March 28, 2024; Revised June 20, 2024; Accepted June 21, 2024)

ABSTRACT. Transition metal complexes are an appealing target in the development of functional materials used frequently in industrial and therapeutic world. The quantum chemical investigations help to obtain a thorough comprehension of the interplay between complexes and biological materials. It necessitates sufficient modeling of chemical phenomena in the system, occasionally involving assistance of classical or semi-empirical computational techniques. Identification of the factors influencing complexes and their optimization is essential for electronic structure calculations and the relevant biochemical potential. The present study aims at correlating analytical studies with the theoretical behavior involving identification of structural features and bonding interactions of the three 4*H*-1-benzopyrans and their spectrophotometrically analyzed palladium complexes using DFT calculations to get acquainted with pharmacological profile of the complexes. FMO studies indicated a higher E_{gap} for ligand in all the cases than their respective Pd(II) complexes. Furthermore, according to the other chemical descriptors, interaction between the ligands and respective complexes, cause chromogenic ligand's chemical hardness to decrease indicating that the formed complexes have lower kinetic stability and more chemical reactivity. Efficiency of the studied ligands further was analyzed by molecular docking against the target proteins, of which 2O0U, a transferase exhibited mutual interactions with all the examined ligands.

KEY WORDS: Palladium(II), 4*H*-1-benzopyran complexes, DFT, MEP, Molecular docking

INTRODUCTION

In recent decades, there has been a surge of interest in the chemistry of transition elements - a rapidly growing and strategically significant area of study. Due to the elements' wide range of industrial applications as alloying elements and the significance of a few of them, especially platinum group metals (PGMs), in biological systems, there is a great deal of interest in the chemistry of these elements [1]. In addition to their inherent significance, these investigations are being propelled more and more by the utilization of transition-metal compounds as solar energy conversion sensitizers [2], phosphorescent dyes for display purposes [3], luminescence-based sensors [4], photocatalyst [5], active elements of electron, photoinitiators [6], electron transfer triggers in biomolecules. Transition metal complexes can be controlled through ligand design and metal selection, exhibiting beautiful colors and rich-excited state behavior. Understanding electronic excited states is crucial in spectroscopic, photophysical, photochemical and theoretical

*Corresponding authors. E-mail: nivagni11@gmail.com; azam_res@yahoo.com

research [7]. Although the behaviour of the metal-organic bond can be highly tuned to achieve desired properties, it is difficult to forecast and hence, calls for a thorough search across a large and intricate space to find the right target for desired applications. The efforts have been made to theoretically study this class through the application of quantum chemical methods. It has been established that driving force behind the development of many quantum chemistry approaches is the intrinsic behaviour of the metal atom at its electronic level.

Palladium, one of the transition metals especially PGMs and a relatively rare platinum metal with atomic number 46, has the widest practical application in various industries, making it a valuable resource. Pallas is the name of a small planet that was discovered in 1802, and it is the source of palladium, and hence its name. The majority of the world's supply of the metal originates from ores that are found in the Soviet Union, Canada, and South Africa. Palladium is a lustrous, ductile, silvery-white metal that melts easily. Palladium is a common alloying element utilized in jewellery. Moreover, palladium also serves as a catalyst. The development of new and improved methods for detection and determination based on sensitive and specific reactions of the elements has been greatly sparked by the study of such a wide range of materials containing trace to high concentrations of palladium [8].

Numerous analytical techniques are available for trace and ultra-trace analysis of elemental composition. Atomic absorption spectrometry (AAS) is the most widely used for trace palladium determination in the parts per million concentration range. Ultra trace element determination requires a more sensitive technique, including potentiometry and voltammetry [9], X-ray [10] and nuclear methods [11]. Electrochemical methods measure free ions and oxidation states. Atomic spectrometric techniques measure total element content but can be affected by the sample matrix. X-ray and nuclear techniques offer low detection limits and matrix insensitivity. Routinely, the determination of trace metals has been carried out by inductively coupled plasma atomic emission spectrometry [12], inductively coupled plasma mass spectrometry [13] electrothermal atomic absorption spectrometry [14], and flame atomic absorption spectrometry [15]. However, there are several drawbacks to the current techniques, such as low sensitivity, a limited pH range, poor temperature control, costly equipment, and large time consumption. Finding an advantageous technique over the limitations of the above-mentioned is highly desirable. Hence, spectrophotometric methods of determination of palladium are mostly preferred as these are cost-effective, easy to handle, and rapid processes with comparable sensitivity, selectivity, and accuracy with good precision [16-25].

Here, our goal is to provide an application of computational chemistry, particularly quantum chemical modeling that has significantly contributed to understanding structure-property relationships and designing inorganic molecules, especially transition metal complexes. Recent advancements in computational chemistry have enabled efficient computation and interpretation of the electronic structures of metal complexes, often based on known structural data. Reliable structure prediction is crucial for predicting molecular properties and designing novel complexes [26]. Quantum chemical methodologies [27], particularly density functional theory (DFT) methods [28], are useful for studying chemical reactivity, analyzing complex reactions, and modeling catalytic reactions. Computational chemistry is widely used by theoreticians and experimental catalysis groups, with results often used to support mechanistic proposals. Modern computational approaches have achieved near-chemical accuracy, with the correlation between molecular modeling results and experimental data becoming a common practice [29].

Not only does computational chemistry help in estimating the structural features and bonding interactions of the compounds in chemistry, but it also helps in estimating and analyzing the biochemical activity and binding affinity of the compounds against a biological target by using a computer-assisted molecular docking study. Molecular docking is a perfect technique to be employed in drug development for the industry to reduce synthesis time and cost while increasing medicine efficacy. It is one of the computational procedures that aims at predicting the precise ligand binding site of its target macromolecule (protein receptors) to form a stable complex [30,

31]. According to Mohapatra *et al.* [32] first, ligand conformations are sampled according to the protein's active site, and then the conformations are ranked according to a scoring function.

The current theoretical study targets the analysis and comparison of the structural quantum chemical features of the 4*H*-1-benzopyrans also named as chromen-4-ones *viz*., 3-hydroxy-2-[2'-(5'-methylthienyl)]-4-oxo-4*H*-1-benzopyran (HMTB), 6-chloro-3-hydroxy-7-methyl-2-(2′-thienyl)-4-oxo-4*H*-1-benzopyran (CHMTB) and 6-chloro-3-hydroxy-7-methyl-2-(2'-furyl)-4-oxo-4*H*-1-benzopyran (CHMFB) and their spectrophotometrically investigated palladium(II) complexes [21-23] using the density functional theory (DFT) method. This study was performed to compare the experimental data to the quantum chemical parameters. Also, with the help of this current study, we can identify the transfer of a ligand in biologically complex systems. By comparing the interaction mechanism of the chelating reagents to the interaction mode of known medications binding to the target protein's active site, molecular docking research assisted in confirming the proper functional group site of the complexing agent for interaction concerning experimentally studied metal centres.

The objectives of this study thus are to highlight the rapid discovery of structure-property relationships in transition-metal chemistry through the integration of computational chemistry and computer science advancements.

COMPUTATIONAL METHODOLOGY

The optimized structural parameters (bond angles and bond lengths) of the title compounds HMTB, CHMTB, and CHMFB were computed by using B3LYP/6-311G++(d,p), whereas complex Pd(II)-HMTB, Pd(II)-HMTB and Pd(II)-CHMFB were calculated by using B3LYP/lanL2DZ.

The selected ligands were docked with the protein receptor molecules in the functional groups of five different proteins, belonging to the classification transferase (2O0U, 5OMY, 6EQ9, 7ORF) [33-36] and signaling protein/inhibitor (6P0I) [37] domains, with the help of Chimera 1.14 [38] and Auto Dock-Vina [37] software. The database was acquired from the protein data bank (RCSB PDB) [40] and the Swiss ADME prediction [41] site made predictions for each of the selected proteins. To find the proteins with the best-fit interactions and the lowest binding energy value, several docking runs have been carried out. The molecule's bioactive nature is shown by its lowest binding energy value [42]. These sampling algorithms help to identify the most energetically favorable conformations of the ligand within the protein's active site, considering their binding mode.

RESULTS AND DISCUSSION

Optimization of Pd(II)-4H-1-benzopyran complexes

DFT studies revealed that all compounds were associated with the C_1 point group. The optimized molecular geometry of all the reagents and their respective Pd(II) complexes is shown in Figure 1, represented by colored atoms and numbering, where red color is for oxygen atom, yellow for sulfur, green for chlorine, grey for carbon, white for hydrogen and greenish blue stands for palladium.

Some of the calculated bond lengths and bond angles for all the compounds shown in Figure 1 have been discussed in Tables 1a and 1b.

Reagent/complexing agent	Complex
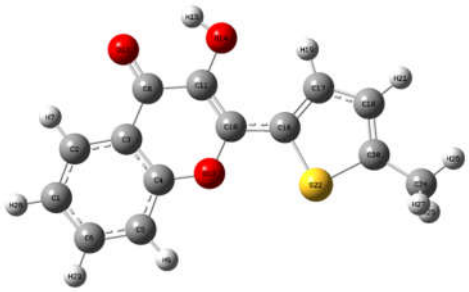 A. HMTB	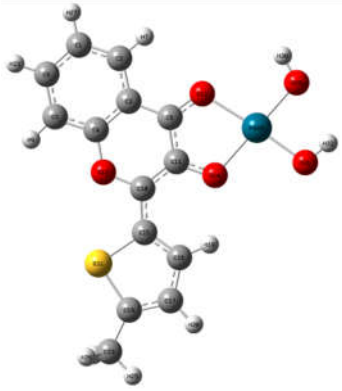 A. Pd(II)-HMTB
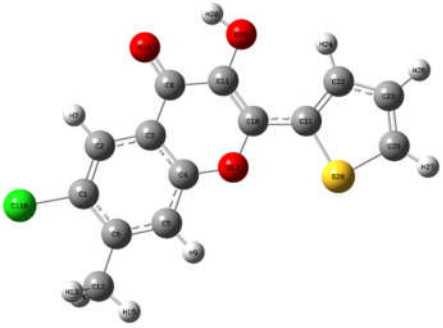 B. CHMTB	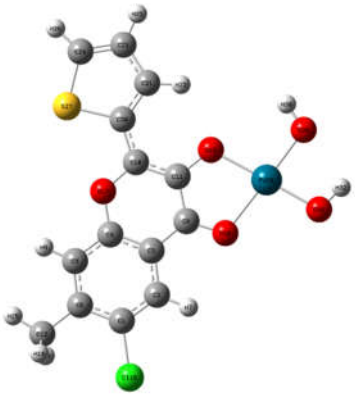 B. Pd(II)-CHMTB
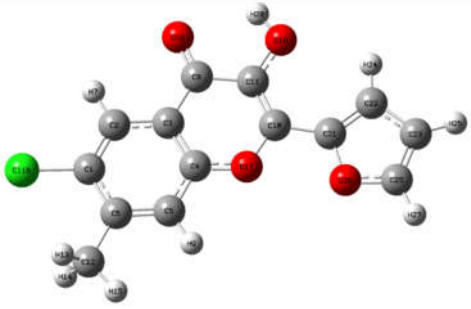 C. CHMFB	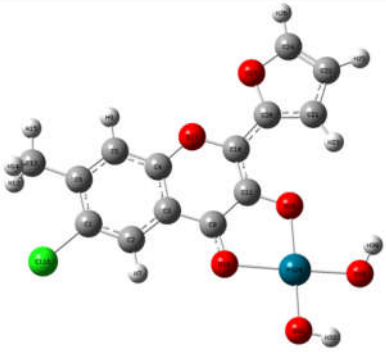 C. Pd(II)- CHMFB

Figure 1. Optimized molecular geometry of [A] HMTB and Pd(II)-HMTB complex; [B] CHMTB and Pd(II)-CHMTB complex; [C] CHMFB and Pd(II)-CHMFB complex.

Table 1a. Optimized geometrical parameters of the reagents [HMTB, CHMTB, CHMFB].

S. No.	Reagents	Parameters	Bond length (Å) B3LYP/ 6-311G++(d,p)	Parameters	Bond angle (º) B3LYP/ 6-311G++(d,p)
1.	HMTB	C8-O13	1.2405	O13-C8-C11	119.2224
		C11-O14	1.3534	C11-O14-H15	104.0965
		C4-O12	1.3625	O14-C11-C10	122.2755
		C10-C16	1.4456	C4-O12-C10	121.1259
		C16- S22	1.7543	O12-C10-C16	112.8927
		O14-H15	0.9789	C16-S22-C20	91.3993
		C20-C24	1.54	C10-C16-S22	120.3082
2	CHMTB	C1-Cl16	1.7482	C2-C1-Cl16	118.6371
		C10-C21	1.4573	O18-C8-C11	120.3096
		C8-O18	1.2045	C11-O19-H20	107.4648
		C11-O19	1.3429	O19-C11-C10	122.0733
		O19-H20	0.9481	C4-O17-C10	121.0802
		C4-O17	1.3398	C21-S28-C25	107.5144
		C21-S28	1.3455	C11-C10-C21	125.2137
3	CHMFB	C1-Cl16	1.76	C2-C1-Cl16	120.0936
		C8-O18	1.2584	O18-C8-C11	121.6228
		C4-O17	1.4423	C11-O19-H20	109.4712
		C11-O19	1.43	O19-C11-C10	119.6773
		O19-H20	0.96	C4-O17-C10	116.7129
		C21-O28	1.4556	C21-O28-C25	102.518
		C10-C21	1.54	C10-C21-O28	124.2552

Table 1b. Optimized geometrical parameters of the Pd(II) complexes [Pd(II)-HMTB, Pd(II)-CHMTB and Pd(II)-CHMFB].

S. No.	Complexes	Parameters	Bond length (Å) B3LYP/lanL2DZ	Parameters	Bond angle (º) B3LYP/lanL2DZ
1	Pd(II)-HMTB	O29-Pd28	1.94	O13-Pd28-O29	114.6921
		O13-Pd28	1.9141	O29-Pd28-O31	103.9782
		O29-H30	0.96	O13-Pd28-O14	95.3967
		C19-C23	1.54	C11-C10-C15	119.0522
		C10-C15	1.4014	C4-O12-C10	117.651
		C4-O12	1.4536	C15-S21-C19	90.8334
		C19-S21	1.7639	C23-C19-C17	124.7645
2	Pd(II)-CHMTB	O29-Pd28	1.94	O19-Pd28-O29	91.1481
		O19-Pd28	1.9518	O29-Pd28-O31	89.0948
		O29-H30	0.96	O19-Pd28-O18	88.6943
		C8-O18	1.2895	C6-C1-Cl16	120.1031
		C1-Cl16	1.7601	C4-O17-C10	117.3224
		C4-O17	1.4555	C20-O27-C24	91.174
		C20-S27	1.7622	C8-C11-O19	116.6839
3	Pd(II)- CHMFB	O29-Pd28	1.94	O19-Pd28-O29	115.6794
		O19-Pd28	1.9113	O29-Pd28-O31	102.8816
		O29-H30	0.96	O19-Pd28-O18	92.3914
		C8-O18	1.2775	C6-C1-Cl16	120.024
		C1-Cl16	1.76	C4-O17-C10	124.6078
		C4-O17	1.3283	C20-O27-C24	106.1168
		C20-O27	1.4358	C8-C11-O19	117.3749

Molecular electrostatic potential (MEP)

The MEP analysis gives an idea regarding the distribution of charge across the 3D molecular surface. The colour grading helps in distinguishing the electron-rich surface areas from the electron-deficient ones [43]. Various physicochemical properties of the title compounds were analyzed on the basis of MEP studies. Figure 2 shows the MEP surface for HMTB and Pd(II)-HMTB, CHMTB, and Pd(II)-CHMTB, CHMFB, and Pd(II)-CHMFB with color variation induced by the difference in charge density. The decreasing magnitude of the electrostatic potential observed is in the following order: blue, green, yellow, orange and finally red. For the given MEP surface, the highest negative potential had been observed at -5.132×10^{-2} a.u (HMTB), -7.66×10^{-2} a.u. [Pd(II)-HMTB complex], -4.83×10^{-2} a.u. (CHMTB), -6.75×10^{-2} a.u. [Pd(II)-CHMTB complex], -5.10×10^{-2} a.u (CHMFB), -6.77×10^{-2} a.u. [Pd(II)-CHMFB complex] (represented by the most intense red color) while the highest positive potential was depicted at 5.132×10^{-2} a.u (HMTB), 7.66×10^{-2} a.u. [Pd(II)- HMTB complex], 4.83×10^{-2} a.u. (CHMTB), 6.75×10^{-2} a.u. [Pd(II)-CHMTB complex], 5.10×10^{-2} a.u. (CHMFB), 6.77×10^{-2} a.u. [Pd(II)-CHMFB complex] (represented by the most intense blue color). As per the MEP, the region with the most intense red color (negative potential) was most prone to electrophilic attack, while the region with the most intense blue color (positive potential) was susceptible to nucleophilic attack. The atoms with a localized lone pair of electrons are generally electronegative centres and represented by reddish-yellow colors depicting negative potential [44]. As seen in Figure 2, the negative electrostatic potential was found over doubly bonded oxygen atoms for HMTB, CHMTB, and CHMFB, whereas it was observed over the hydroxide group bonded with Pd (II) atom for Pd(II)-HMTB, Pd(II)-CHMTB and Pd(II)-CHMFB complexes. On the other hand, the lesser positive electrostatic potential was depicted over the hydrogen atoms bonded to the aryl carbon atoms of the rings.

FMO HOMO-LUMO energy gap

The HOMO to LUMO energy band gap can be used to analyze the compound's stability, chemical activity, and other variables. The chemical reactivity indices like chemical hardness, electronegativity, electronic chemical potential, and electrophilicity index, were calculated for the title compound using the energy values of HOMO and LUMO [45]. The various relevant pairs of molecular orbitals along with the energy gap between HOMO and LUMO is 3.56 eV (HMTB), 4.24 eV (CHMTB), 9.71 eV (CHMFC), 1.22 eV (Pd(II)-HMTB), 2.76 eV (Pd(II)-CHMTB) and 2.51 eV (Pd(II)- CHMFC) are as shown in Figure 3, and this is also an important parameter for determining the electron conductivity. Chemical hardness is an indication of the stability and reactivity of a chemical system.

This descriptor is used as a measure of resistance to change in the electron distribution or charge for the given molecule. As shown in Table 2, the molecule's chemical hardness was calculated to be 1.78 eV (HMTB), 2.12 eV (CHMTB), 4.86 eV (CHMFB), 0.61 eV [Pd(II)-HMTB complex], 1.38 eV [Pd(II)-CHMTB complex] and 1.26 eV [Pd(II)-CHMFB complex]. A reasonably high value indicates the substance is chemically stable or very close to its stability. The electronegativity value, which measures the power of an atom in a molecule to attract electrons towards it was found to be 4.07 eV (HMTB), 4.15 eV (CHMTB), 4.11 eV (CHMFB), 2.9 eV [Pd(II)-HMTB complex], 4.79 eV [Pd(II)-CHMTB complex] and 5.03 eV [Pd(II)-CHMFB complex]. The electrophilicity index which measures the ability of a molecular species to soak up electrons was found to be 4.65 eV (HMTB), 4.06 eV (CHMTB), 1.74 eV (CHMFB), 6.89 eV [Pd(II)-HMTB complex], 8.31 eV [Pd(II)-CHMTB complex] and 10.04 eV [Pd(II)-CHMFB complex]. The electrophilicity index has also been found to be useful in predicting toxicological behavior. And finally, the computed value for the chemical softness is 0.56 eV (HMTB), 0.47 eV (CHMTB), 0.21 eV (CHMFB), 1.64 eV [Pd(II)-HMTB complex], 0.72 eV [Pd(II)-CHMTB complex] and 0.79 eV [Pd(II)-CHMFB complex] and is thus predicted to have very low toxicity [46].

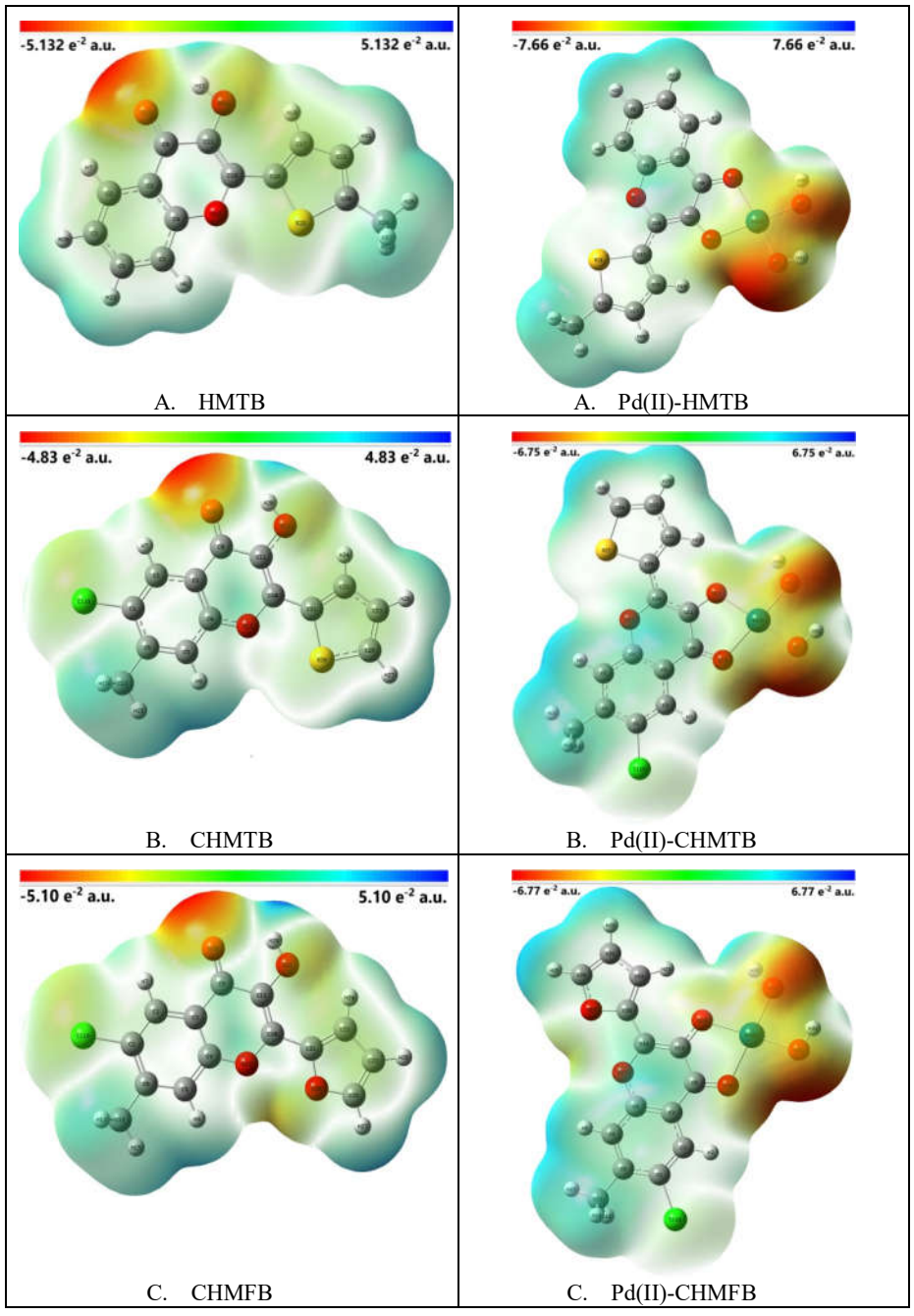

Figure 2. Molecular electrostatic potential (MEP) of [A] HMTB and Pd(II)-HMTB complex; [B] CHMTB and Pd(II))-CHMTB complex; [C] CHMFB and Pd(II)-CHMFB complex.

Table 2. Calculated energy values of the studied reagents and their palladium(II) complexes.

Parameters	Energy values					
	Reagents B3LYP/6-311++G(d,p) method			Complexes B3LYP/lanL2DZ method		
	HMTB	CHMTB	CHMFB	Pd(II)-HMTB	Pd(II)-CHMTB	Pd(II)-CHMFB
E_{HOMO} (eV)	-5.85	-6.27	-8.96	-2.29	-6.17	-6.28
E_{LUMO} (eV)	-2.29	-2.03	0.75	-3.51	-3.41	-3.77
Ionization potential (eV)	5.85	6.27	8.96	2.29	6.17	6.28
Electron affinity (eV)	2.29	2.03	-0.75	3.51	3.41	3.77
Energy gap (eV)	3.56	4.24	9.71	1.22	2.76	2.51
Electronegativity (eV)	4.07	4.15	4.11	2.9	4.79	5.03
Chemical potential (eV)	-4.07	-4.15	-4.11	-2.9	-4.79	-5.03
Chemical hardness (eV)	1.78	2.12	4.86	0.61	1.38	1.26
Chemical softness (eV)	0.56	0.47	0.21	1.64	0.72	0.79
Electrophilicity index (eV)	4.65	4.06	1.74	6.89	8.31	10.04

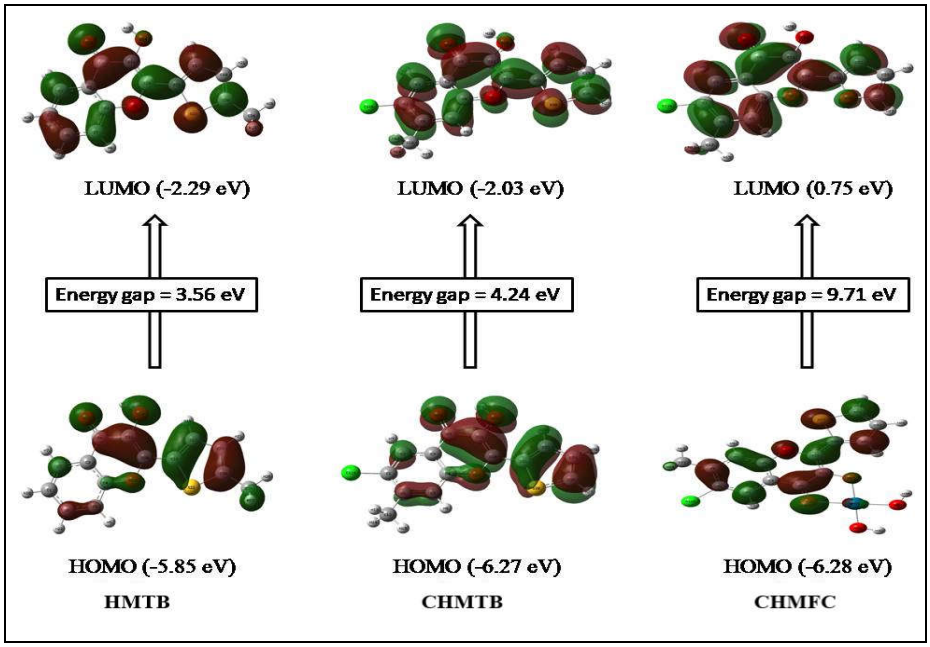

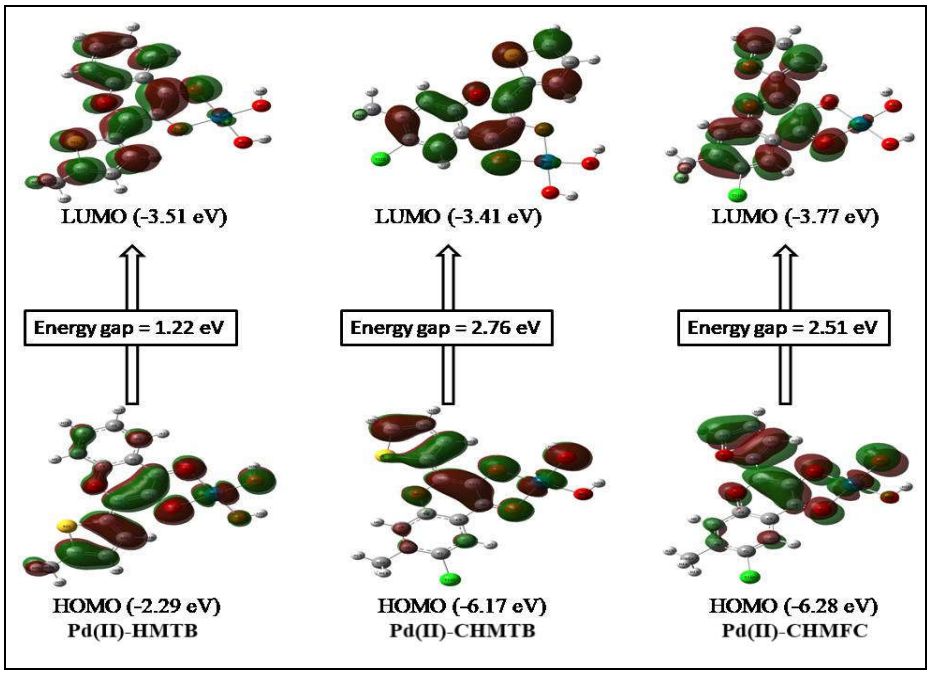

Figure 3. Atomic orbital HOMO–LUMO composition of the frontier molecular orbital and energy gap of the studied reagents and corresponding Pd(II) complexes.

Table 3. Docking Analysis data of ligands [A-HMTB; B-CHMTB; C-CHMFB] with different proteins.

	Ligands	Proteins				
		2O0U	5OMY	6EQ9	6P0I	7ORF
Residue		3	3	3	3	3
Binding score (k cal/mol)	A	-8.7	-8.4	-8.2	-8.1	-7.9
	B	-8.7	-8.3	-8.0	-8.2	-8.0
	C	-8.1	-7.9	-7.6	-7.7	-8.0
H-bond distance and residue involved in H-bonding	A	2.60	2.62 (ASN 118, VAL 116)	2.37, 2.50 (MET 149)	2.31 (TYR 43)	1.82
	B	2.32	--	2.51	3.31, 2.28 (TYR 43)	3.34, 1.91
	C	--	--(ASN 118)	2.34 (ASN 152)	2.65 (ASN 127)	3.12
Residue involved in other non-	A	ILE 70, LYS 93, MET 146, LEU 206, VAL 196, VAL 78	ARG 172, ILE 95, ILE 174, VAL 53,VAL 66, MET 163	ILE 70, LEU 206, LYS 93, MET 146, VAL 78, ALA 91, VAL 196	LYS 128, PHE 39, ALA 158, PRO 45, ALA 29	MET 146, ALA 91, VAL 78, LEU 206, ILE 70, VAL 196, LYS 93
	B	ILE 70, MET 146, LEU 206, VAL 78	VAL 116, VAL 66, ILE 95, ARG 172, MET 163,	ILE 70, LEU 206, LYS 93, MET 146, ALA 91,	PHE 39, LYS 128, ALA 158, ALA 29,	MET 146, LYS 93, VAL 78, ALA 91 ILE

covalent interactions			VAL 53, ILE 174, ASN 118	VAL 196, VAL 78	SER 28, PRO 45	70, VAL 196, LEU 206
	C	MET 146, VAL 78, LEU 206, VAL 196, ALA 91, ILE 70, ILE 124, MET 115, LEU 126, LEU 144, LYS 93	LEU 45, VAL 53, MET 163, VAL 66, ILE 95, VAL 116,ARG 172	VAL 196, ILE 70, ALA 91, LEU 206, VAL 78, LYS 93	LYS 128, PHE 39, ALA 158, LYS 159, LEU 131, ALA 29	MET 146, ALA 91, VAL 78, VAL 196, ILE 70, ILE 124, LEU 206, LEU 126, LEU 144

Molecular docking

Furthermore, using molecular docking against target proteins, the efficiency of the studied ligands was analyzed and discussed. The least binding energies (kcal/mol), H-bond distance, and residue involved in other non-covalent interactions obtained by docking analysis of molecules were represented in tabulated form (Table 3). In all the protein receptors, 2O0U showed the least energy of binding at -8.7 kcal/mol for ligands HMTB (A) and CHMTB (B), whereas -8.1 kcal/mol for CHMFB (C) and this was the most docked proteins among all that interacted with the ligands. 2D-plotting of docked complexes for identifying the other non-covalent interactions other than H-bond along with residue involved in it were done by using Biovia discovery studio tool [47]. This receptor protein consists of 3 residue and hydrogen bonds possessing H-bond lengths of 2.60 and 2.32 Å for ligands A and B, respectively. All the three compounds A, B and C were found to interact with various different receptors and its other non-covalent interactions were as depicted in Figures 4, 5, 6 and 7. The least value of binding energy shows that the protein 2O0U is the potentially active compound which properly interacted with all the three described ligands A, B and C.

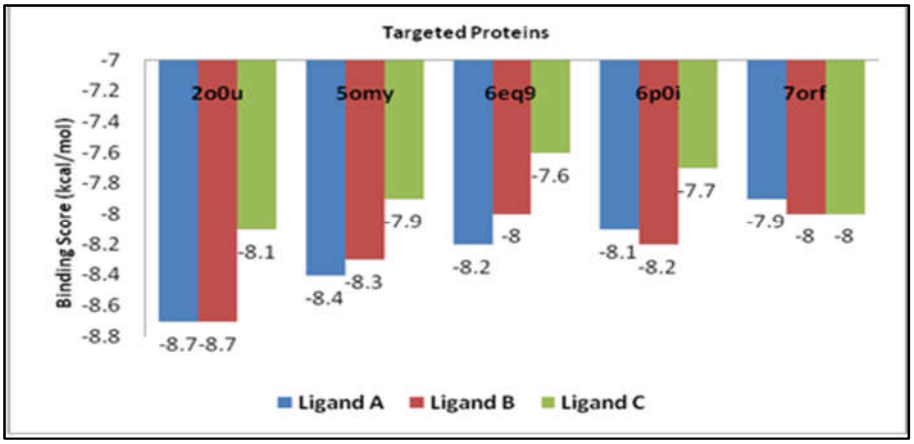

Figure 4. The binding energy values of the ligands, HMTB (A), CHMTB (B) and CHMFC (C) against five different proteins.

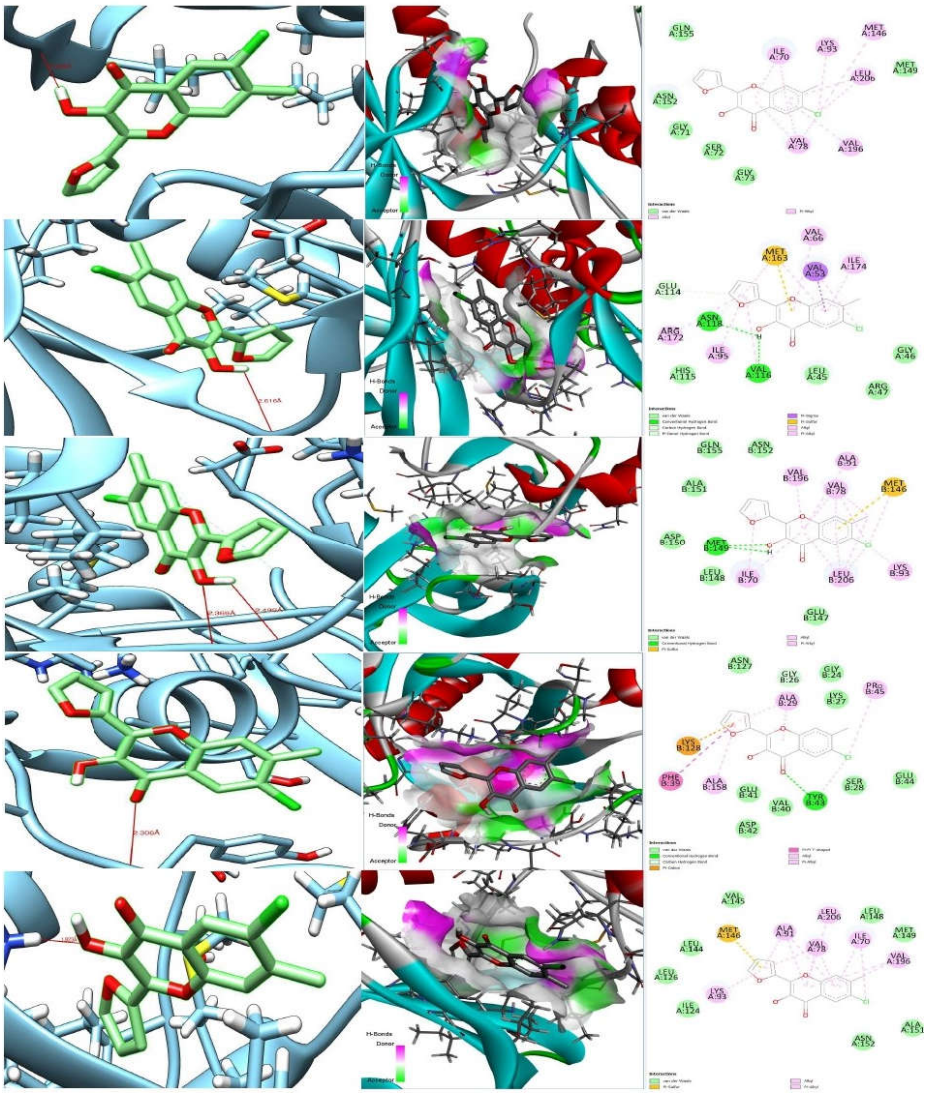

Figure 5. 3D orientations of HMTB [ligand A] in the active site of the selected proteins.

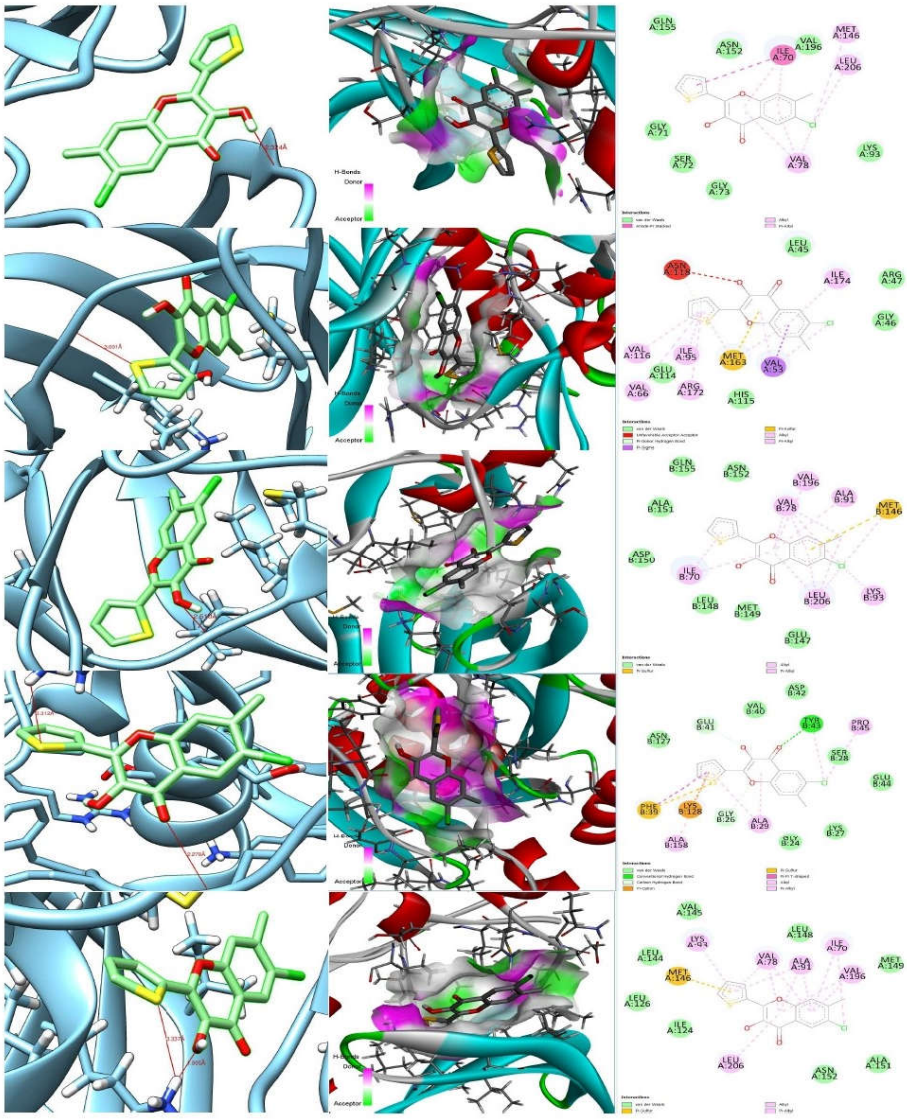

Figure 6. 3D orientations of CHMTB [ligand B] in the active site of the selected proteins.

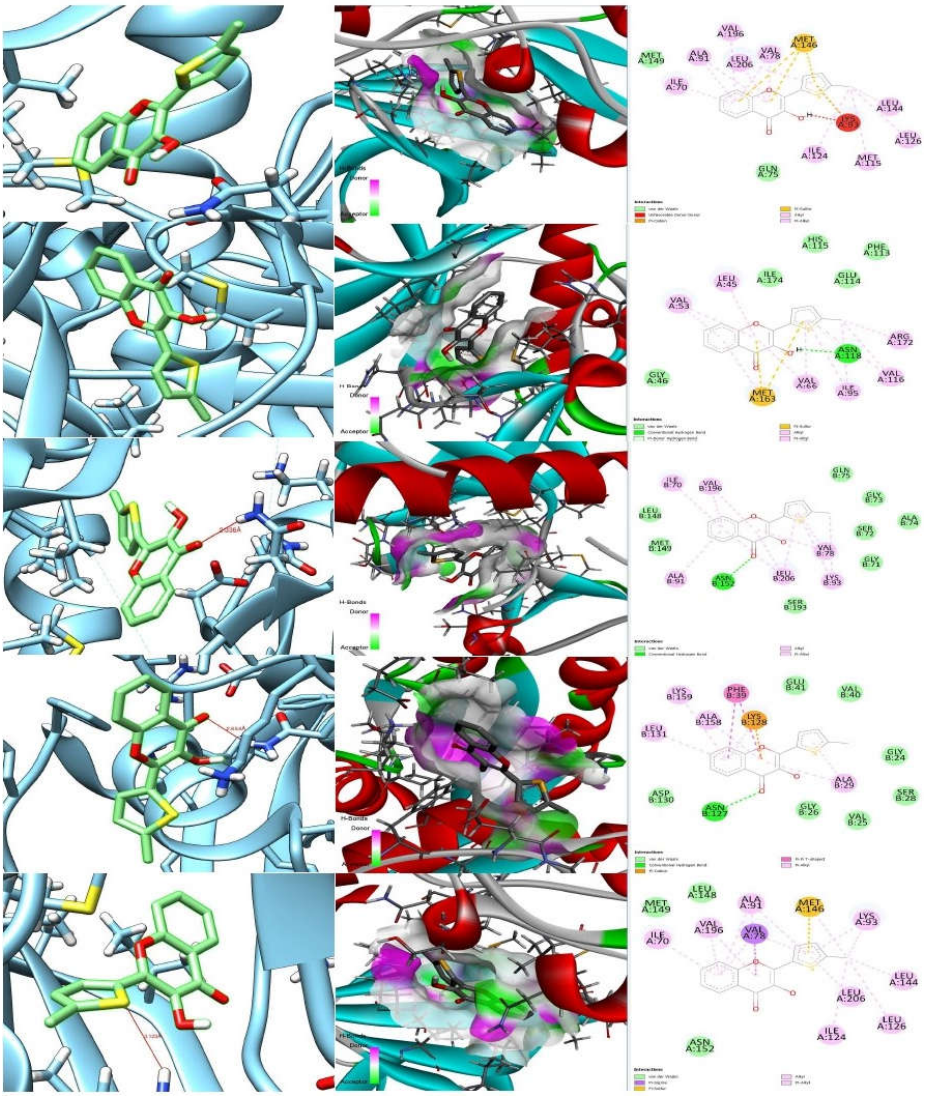

Figure 7. 3D orientations of CHMFB [ligand C] in the active site of the selected proteins.

CONCLUSION

In coordination compounds, the transition metals have the unusual ability to cause notable alterations in the electronic structure of the ligands involved, frequently resulting in a dramatic alteration in their chemical and biological behavior. This ability helps to explain how they have evolved into living systems. The intricacy of the behaviour of metal atom at the electronic level

is the driving force behind the development of many quantum chemistry approaches for their explanation. The present study incorporates a theoretical study with satisfactory results of the 4*H*-1-benzopyrans exhibiting unique chelating and biological properties towards palladium in its divalent state. The chelating efficacy of the selected bidentate ligands *viz*. 3-hydroxy-2-[2'-(5'-methylthienyl)]-4-oxo-4*H*-1-benzopyran (HMTB), 6-chloro-3-hydroxy-7-methyl-2-(2′-thienyl)-4-oxo-4*H*-1-benzopyran (CHMTB) and 6-chloro-3-hydroxy-7-methyl-2-(2'-furyl)-4-oxo-4*H*-1-benzopyran (CHMFB) shown by coordinating the 4*H*-1-benzopyran rings to palladium(II) centers as described in our previous analytical research [21-23], when extended to DFT calculations generated the ideal and optimized complex structures. The existence of electron density around the pyran ring in the three mentioned ligands and around the core metal atom in their respective Pd(II) complexes has also been amply demonstrated by the MEP structures both for the ligands and their bivalent metal complexes, supporting the presence of coordinating sites. Although, all the three selected benzopyrans were able to interact with different protein receptors as indicated during molecular docking studies with respect to five variable proteins as 2O0U, 5OMY, 6EQ9, 7ORF and 6P0I belonging to different domains, yet, the protein 2O0U interacted properly with all the three described ligands as is indicated by the least value of binding energy, hence exhibited mutual interactions with all the three examined ligands.

ACKNOWLEDGMENTS

The authors acknowledge the financial support through the Research Supporting Project number (RSP2024R147), King Saud University, Riyadh, Saudi Arabia. Sincere thanks are due to the authorities, MMEC, Maharishi Markandeshwar (Deemed to be University), Mullana for providing the required facilities to carry out the presented work. Appreciations are also due to Dr. Navneet Kaur, 1st PhD student of NA.

REFERENCES

1. Elatter, R.H.; El-Malla, S.F.; Kamal, A.H.; Mansour, F.R. Applications of metal complexes in analytical chemistry: A review article. *Chem. Rev.* **2024**, 501, 215568.
2. Pawlus, K.; Jarosz, T. Transition metal coordination compounds as novel materials for dye-sensitized solar cells. *Appl. Sci.* **2022**, 12, 3442.
3. Chou, P.-T.; Chi, Y. Phosphorescent dyes for organic light-emitting diodes. *Chem. Eur. J.* **2007**, 13, 380-395.
4. Sathish, V.; Ramdass, A.; Velayudham, M.; Lu, K.-L.; Thanasekaran, P.; Rajagopal, S. Development of luminescent sensors based on transition metal complexes for the detection of nitroexplosives. *Dalton Trans.* **2017**, 46, 16738-16769.
5. Cieśla, P.; Kocot, P.; Mytych, P.; Stasicka, Z. Homogeneous photocatalysis by transition metal complexes in the environment. *J. Mol. Catal. A Chem.* **2004**, 224, 17-33.
6. Ferraro, V.; Adam, C.R.; Vranic, A.; Bräse, S. Recent advances of transition metal complexes for photopolymerization and 3D printing under visible light. *Adv. Funct. Mater.* **2023**, 34, 2302157.
7. Çapkın, A.; Pişkin, M.; Durmuş, M.; Bulut, M. Spectroscopic, photophysical and photochemical properties of newly metallo-phthalocyanines containing coumarin derivative. *J. Mol. Struct.* **2020**, 1213, 128145.
8. Kaur, N.; Agnihotri, N.; Agnihotri, R.; Sharma, R.K. A treatise on spectrophotometric determination techniques of palladium(II) ions. *J. Chem. Rev.* **2022**, 4, 81-99.
9. Richard, J.C.B.; Milton, M.J.T. Analytical techniques for trace element analysis: an overview, *Trends Anal. Chem.* **2005**, 24, 266-274.

10. Marinkovic, N.S.; Sasaki, K.; Adzic, R.R. Determination of single- and multi-component nanoparticle sizes by X-ray absorption spectroscopy. *J. Electrochem. Soc.* **2018**, 165, J3222-J3230.
11. Das, D.D.; Sharma, N.; Chawla, P.A. Neutron activation analysis: An excellent nondestructive analytical technique for trace metal analysis. *Crit. Rev. Anal. Chem.* 2023, 1-17.
12. Pehlivana, E.; Arslanb, G.; Godec, F.; Altuna, T.; Özcand, M.M. Determination of some inorganic metals in edible vegetable oils by inductively coupled plasma atomic emission spectroscopy (ICP-AES). *Grasas Aceites* **2008**, 59, 239-244.
13. Liu, K.; Gao, X.; Li, L.; C.-T.A.; Chen, Xing, Q. Determination of ultra-trace Pt, Pd and Rh in seawater using an off-line pre-concentration method and inductively coupled plasma mass spectrometry, *Chemosphere* **2018**, 212, 429-437.
14. Burylin, M.Y.; Pupyshev, A.A. Development of electrothermal atomic absorption spectrometry in 2005-2016. *J. Anal. Chem.* **2017**, 72, 935-946.
15. D'souza, M.D.; Dwivedi, P.; Lokhande, R.; Anvekar, T.; D'souza, A.J. Simple, sensitive and easy to use, method for determination of palladium content in palladium acetate using flame atomic absorption spectrophotometry. *Orient. J. Chem.* **2021**, 37, 880-884.
16. Bulska, E.; Ruszczyńsa, A. Analytical techniques for trace element determination. *Phys. Sci. Rev.* **2017**, 2, 20178002.
17. Barhate, V.D.; Madan, P.; Gupta, A.K.S.; Mandharev, D.B. Extractive spectrophotometric determination of palladium(II) with isonitroso *p*-nitroacetophenonethiosemicarbazone (HINATS). *Orient. J. Chem.* **2009**, 25, 731-733.
18. Mathew, B.; Mini, V.; Deepthi, B. Spectrophotometric determination of palladium(II) using a nitrogen, sulphur and oxygen donor triazine. *Orient. J. Chem.* **2010**, 26, 233-238.
19. Karthikeyan, J.; Naik, P.P.; Shetty, A.N. Analytical properties of *p*-[N,N-bis(2-chloroethyl) amino]benzaldehydethiosemicarbazone: Spectrophotometric determination of palladium(II) in alloys, catalysts, and complexes. *Environ. Monit. Assess.* **2011**, 173, 569-577.
20. Bagal, M.R.; Shaikh, U.P.K.; Sakhre, M.A.; Vaidya, S.R.; Lande, M.K.; Arbad, B.R. Spectrophotometric determination of *N*-decylpyridine-4-amine from malonate media. *J. Indian Chem. Soc.* **2014**, 91, 845-851.
21. Kaur, N.; Agnihotri, N.; Agnihotri, R. 3-Hydroxy-2-[2'-(5'-methylthienyl)]-4-oxo-4*H*-1-benzopyran for the spectrophotometric determination of tungsten(VI) and palladium(II), *Vietnam J. Chem.* **2019**, 57, 686-695.
22. Kaur, N.; Agnihotri, N.; Berar, U. Microdetermination of palladium(II) using 6-chloro-3-hydroxy-7-methyl-2-(2′-thienyl)-4-oxo-4*H*-1-benzopyran. *Asian J. Chem.* **2020**, 32, 1597-1602.
23. Kaur, N.; Agnihotri, R.; Agnihotri, N. Studies on the liquid phase extraction and spectrophotometric determination of 6-chloro-3-hydroxy-methyl-2-(2'-furyl)-4*H*-chromen-4-one complex of palladium(II). *Rasayan J. Chem.* **2022**, 15, 262-268.
24. Tymoshuk, O.S.; Frdyshyn, O.S.; Oleksiv, L.V.; Rydchuk, P.V.; Matiychuk, V.S. Spectrophotometric determination of palladium(II) ions using a new reagent: 4-(N'-(4-Imino-2-oxo-thiazolidine-5-ylidene)-hydrazino)-benzoic Acid (*p*-ITYBA). *J. Chem.* **2020**, 2020, 1–8.
25. Agnihotri, N.; Rathi, P.; Agnihotri, R.; Kumar, V.; Shiwani, S. Molecular dynamics, biological study and extractive spectrophotometric determination of vanadium (V) -2-methyl-8-quinolinol complex. *IJCCE* **2021**, 40, 207-214.
26. Nandy, A.; Daun, C.; Taylor, M.G.; Liu, F.; Steeves, A.H.; Kulik, H.J. Computational discovery of transition-metal complexes: from high-throughput screening to machine learning. *Chem. Rev.* **2021**, 121, 9927-10000.
27. Agnihotri, N.; Mohini; AI-Resayes, S.I.; Javed, S.; Azam, M.; Saurav, K.; Muthu, S.; Kumar, V.; Singh, M. A spectrophotometric determination and the quantum chemical investigation of

Pd(II)-3-hydroxy-2-(4-methoxyphenyl)-4-oxo-*4H*-1-benzopyran complex. *Bull. Chem. Soc. Ethiop.* **2024**, 38, 591-603.
28. Mohamad, H.A.; Ali, K.O.; Gerber, T.A.; Hosten, E.C. Novel palladium(II) complex derived from mixed ligands of dithizone and triphenyllphosphine synthesis, characterization, crystal structure, and DFT study. *Bull. Chem. Soc. Ethiop.* **2022**, 36, 617-626.
29. Bogojeski, M.; Vogt-Maranto, L.; Tuckerman, M.E.; Müller, K.R.; Burke, K. Quantum chemical accuracy from density functional approximations via machine learning. *Nat. Commun.* **2020**, 11, 5223.
30. Garima, Km.; Fatima, A.; Pooja, Km.; Sandhya, S.; Sharma, M.; Kumar, M.; Muthu, S.; Siddiqui, N.; Javed, S. Quantum computational, spectroscopic, Hirshfeld surface analysis of 3-picoline (monomer and dimer) by DFT/TD-DFT with different solvents, molecular docking, and molecular dynamic studies. *Polycycl. Aromat. Compd.* **2022**, 43, 1-25.
31. Fatima, A.; Khanum, G.; Sharma, A.; Garima, Km.; Savita, S.; Verma, I.; Siddiqui, N.; Javed, S. Computational, spectroscopic, Hirshfeld surface, electronic state and molecular docking studies on phthalic anhydride. *J. Mol. Struct.* **2022**, 1249, 131571.
32. Mohapatra, R.; Mallick, S.; Nanda, A.; Sahoo, R.N.; Pramanik, A.; Bose, A.; Das, D.; Pattnaik, L. Analysis of steady state and non-steady state corneal permeation of diclofenac. *RSC Adv.* **2016**, 6, 1976-31987.
33. Angell, R.M.; Atkinson, F.L.; Brown, M.; Chuang, T.T.; Christopher, J.A.; Cichy-Knight, M.; Dunn, A.K.; Hightower, K.E.; Malkakorpi, S.; Musgrave, J.R.; Neu, M.; Rowland, P.; Shea, R.L.; Smith, J.L.; Somers, D.O.; Thomas, S.A.; Thompsona, G.; Wang, R.N-(3-Cyano-4,5,6, 7-tetrahydro-1-benzothien-2-yl)amides as potent, selective, inhibitors of JNK2 and JNK3. *Bioorg. Med. Chem. Lett.* **2007**, 17, 1296-1301.
34. Hochscherf, J.J.; Lindenblatt, D.; Witulski, B.; Birus, R.; Aichele, D.; Marminon, C.; Bouaziz, Z.; Borgne, M.L.; Jose, J.; Niefind, K. Unexpected binding mode of a potent indeno[1,2-b]indole-type inhibitor of protein kinase CK2 revealed by complex structures with the catalytic subunit CK2α and its paralog CK2α. *Pharmaceuticals* **2017**, 10, 1-19.
35. Ansideri, F.; Macedo, J.T.; Eitel, M.; El-Gokha, A.; Zinad, D.S.; Scarpellini, C.; Kudolo, M.; Schollmeyer, D.; Boeckler, F.M.; Blaum, B.S.; Laufer, A.S.; Koch, P. Structural optimization of a pyridinylimidazole scaffold: Shifting the selectivity from p38α mitogen-activated protein kinase to c-Jun N-terminal kinase 3. *ACS Omega* **2018**, 3, 7809-7831.
36. Bum-Erdenea, K.; Liua, D.; Gonzalez-Gutierrezb, G.; Ghozayela, M.K.; Xua, D.; Meroueh, S.O. Small-molecule covalent bond formation at tyrosine creates a binding site and inhibits activation of Ral GT Pases. *PNAS* **2020**, 117, 7131-7139.
37. Reynders, M.; Chaikuad, A.; Berger, B.; Bauer, K.; Koch, P.; Laufer, S.; Knapp, S.; Trauner, D. Controlling the covalent reactivity of a kinase inhibitor with light. *Angew. Chem. Int. Ed.* **2021**, 60, 20178-20183.
38. Pettersen, E.F.; Goddard, T.D.; Huang, C.C.; Couch, G.S.; Greenblatt, D.M.; Meng, E.C.; Ferrin, T.E. UCSF chimera? A visualization system for exploratory research and analysis. *J. Comput. Chem.* **2004**, 25, 1605-1612.
39. Eberhardt, J.; Santos-Martins, D.; Tillack, A.F.; Forli, S. AutoDockVina 1.2.0: New docking methods, expanded force field and python bindings. *J. Chem. Inf. Model.* **2021**, 61, 3891-3898.
40. Berman, H.M.; Henrick, K.; Nakamura, H. Announcing the worldwide protein data bank, *Nat. Struct. Biol.* **2003**, 10, 980.
41. Daina, A.; Michielin, O.; Zoete, V. Swiss target prediction: updated data and new features for efficient prediction of protein targets of small molecules. *Nucleic Acids Res.* **2019**, 47, W357-W364.
42. Pooja, Km.; Fatima, A.; Sharma, A.; Garima, Km.; Savita, S.; Kumar, M.; Verma, I.; Siddiqui, N.; Javed, S. Experimental, theoretical, Hirschfeld surface, electronic excitation and

molecular docking studies on fomepizole(4-methyl-1H-pyrazole). *J. Mol. Struct.* **2022**, 1256, 132549.
43. Suresh, C.H.; Remya, G.S.; Anjalikrishna, P.K. Molecular electrostatic potential analysis: A powerful tool to interpret and predict chemical reactivity. *Wiley Interdiscip. Rev. Comput. Mol. Sci.* **2022**, 12, e1601.
44. Akman, F. Experimental and theoretical investigation of molecular structure, vibrational analysis, chemical reactivity, electrostatic potential of benzyl methacrylate monomer and homopolymer. *Can. J. Phys.* **2016**, 94, 853–864.
45. Sheela, N.R.; Muthu, S.; Sampathkrishnan, S. Molecular orbital studies (hardness, chemical potential and electrophilicity), vibrational investigation and theoretical NBO analysis of 4-40-(1H-1,2,4-triazol-1-yl methylene) dibenzonitrile based on abinitio and DFT methods, *Spectrochim. Acta A Mol. Biomol. Spectrosc.* **2014**, 120, 237-251.
46. Hussein, Y.T.; Azeez, Y.H. DFT analysis and *in silico* exploration of drug-likeness, toxicity prediction, bioactivity score, and chemical reactivity properties of the urolithins, *J. Biomol. Struct. Dyn.* **2023**, 41, 1168-1177.
47. Systemes D. BIOVIA discovery studio, **2016**.